International Journal of Heat and Fluid Flow 30 (2009) 54–65

Contents lists available at ScienceDirect

International Journal of Heat and Fluid Flow

journal homepage: www.elsevier.com/locate/ijhff

A new extension for k–ω turbulence models to account for wall roughness

Tobias Knopp [a,*], Bernhard Eisfeld [b], Javier Bartolome Calvo [b]

[a] DLR (German Aerospace Center), Institute of Aerodynamics and Flow Technology, Bunsenstr. 10, 37073 Göttingen, Germany
[b] DLR (German Aerospace Center), Institute of Aerodynamics and Flow Technology, Lilienthalplatz 7, 38108 Braunschweig, Germany

ARTICLE INFO

Article history:
Received 23 July 2007
Received in revised form 16 July 2008
Accepted 23 September 2008
Available online 21 November 2008

Keywords:
Boundary layer
Turbulence modelling
Wall roughness
Equivalent sand grain
Skin friction

ABSTRACT

This paper presents a new extension for k–ω turbulence models to account for surface roughness for transitionally and fully rough surfaces. It is based on the equivalent sand grain approach and accounts for theoretical considerations on the log-layer solution for fully rough surfaces. An appropriate behaviour for transitional roughness is achieved by means of wall values for k and ω which depend on the roughness Reynolds number. In the limit of vanishing roughness, the smooth wall boundary condition is recovered. For the full range of roughness Reynolds numbers the new roughness modification gives very successful predictions for a variety of flat plate turbulent boundary layer flows and for the pipe flow experiments by Nikuradse. The new method allows for the simulation of flows over rough surfaces at the same grid resolution requirements as for smooth walls. Thereby the extremely fine near-wall mesh resolution required by the Wilcox roughness modification is avoided. Secondly the new roughness modification gives significantly improved predictions in skin friction for transitional roughness Reynolds numbers compared to the roughness extension by Wilcox. Thirdly, the new roughness extension does not require a modification of the SST k–ω model, whereas a modification is necessary if the roughness extension by Wilcox is used. Finally the new method is applied successfully to predict the aerodynamic effects of surface roughness on the flow past an airfoil in highlift conditions.

1. Introduction

Most wall-bounded flows of engineering interest are turbulent in character. In many situations at least parts of the surface are rough, e.g., aerodynamic flows over airfoils with icing or turbine blades with surface roughness due to manufacturing imperfections or as a longterm result of erosion by impinging combustor air.

The accurate and reliable prediction of the effects of surface roughness on fluid flow and heat transfer are of great interest for engineers using CFD as a major design tool. A survey on different approaches for turbulence model modifications to account for surface roughness can be found e.g., in Patel (1998), and Aupoix and Spalart (2003). In the present paper, the "equivalent sand grain approach" is considered, which is due to the work of Nikuradse (1933). This approach uses a theoretical roughness length called equivalent sand grain roughness. Nikuradse performed experiments with pipes with sand glued to the wall as densely as possible, and for the equivalent sand grain size he used the size of the sieve. If surface roughness comes from regular arrays of discrete three-dimensional roughness elements of a certain geometry such as cones, hemispheres, etc., or from a stochastic roughness distribution, then the corresponding equivalent sand grain roughness height has to be computed from the real, geometrical roughness size using an empirical correlation, see e.g. Schlichting (1968), Dirling (1973).

The experimental data by Nikuradse are still of immeasurable value for the design and validation of roughness modifications for turbulence models. In pipe flow, friction is related to the drop in pressure over an axial distance, which can be measured very accurately. Nikuradse proposed empirical relations for the skin friction (to be more precise: for the friction factor) and for the shift of the velocity profile in the logarithmic layer as a function of the equivalent sand grain roughness. Moreover, experimental results from several research groups for flat plate turbulent boundary layer flow with surface roughness provide additional data for skin friction and partially also for the shift of the log-layer profiles for velocity.

For boundary layers over flat plates with surface roughness, local skin friction coefficients are determined from the Reynolds shear stresses and mean velocities, measured at a distance above the crests of the roughness elements where $-\overline{u'v'}/u_\infty^2$ is 96–98% of $c_f/2$. Using hot-wire anemometry, the uncertainty in $-\overline{u'v'}$ and thus in c_f is about $\pm 10\%$, see Ligrani and Moffat (1986) and references therein.

In computational models which use the equivalent sand grain approach, the rough surface is replaced by an effective, smooth surface, on which modified boundary conditions are imposed. For

* Corresponding author. Tel.: +49 551 7092451; fax: +49 551 7092416.
E-mail address: Tobias.Knopp@dlr.de (T. Knopp).

0142-727X/$ - see front matter © 2008 Elsevier Inc. All rights reserved.
doi:10.1016/j.ijheatfluidflow.2008.09.009

Nomenclature

B	shift in the log-law for rough walls
C	shift in the log-law for smooth walls, $C = 5.1$
c	airfoil chord length
c_f	skin friction coefficient $c_f = \tau_w/((1/2)\rho u_\infty^2)$
d_0	offset in the wall distance to account for wall roughness
L	length of the flat plate (in [m])
k	turbulent kinetic energy in the k–ω model
k_r	equivalent sand grain roughness height
R	radius of the pipe in Nikuradse experiments
u	streamwise velocity component
u_τ	friction velocity
x	streamwise position for flow over flat plate (in [m])
y	distance to the nearest wall

Greeks

α	angle of incidence for airfoil flows
β_k	constant in the k–ω model, $\beta_k = 0.09$
κ	von Kármán constant
ν	kinematic viscosity
ν_t	eddy or turbulent viscosity
ρ	density
τ_w	wall shear stress
ω	turbulence frequency in the k–ω model

Subscripts, superscripts

$+$	variable in wall scaling
CL	centerline velocity in pipe flow
∞	freestream value
w	wall value

Abbreviations

RANS	Reynolds averaged Navier–Stokes equations
SA model	Spalart–Allmaras turbulence model

low-Re turbulence models see Aupoix and Spalart (2003), Durbin et al. (2001) and for wall-functions see Suga et al. (2006) and references therein. The design of roughness modifications has to ensure both (i) predictions of c_f close to experimental data and (ii) prediction of profiles for velocity and turbulence quantities in agreement with experimental results and empirical theory. For fully rough surfaces, the design of roughness modifications can be guided by theoretical considerations regarding the log-layer solution, see e.g. Kays and Crawford (1993) pp. 230. On the other hand, regarding the near-wall behaviour of mean velocity and turbulence quantities, the available experimental data are very limited and at present no successful empirical relations exist.

Recently, two extensions of the Spalart–Allmaras turbulence model (abbreviated SA model) to account for wall roughness have been proposed, developed independently by Boeing and ONERA, see Aupoix and Spalart (2003). The underlying ideas used for the SA model are valuable also for the design of roughness modifications for other low-Re RANS turbulence models. The two roughness modifications yield similar predictions, and are in fair agreement with experimental data. In this paper, only the Boeing approach is considered, as it is very suitable for parallel, unstructured CFD methods.

A rough wall modification for the two layer k-ϵ model has been proposed in Durbin et al. (2001). The approach uses a calibration procedure for transitional roughness values. Thereby the model is designed to predict the shift of the log-layer profiles for velocity in agreement with the empirical relation by Ligrani and Moffat (1986).

An alternative approach was pursued by Suga et al. (2006), who proposed an analytical wall-function for turbulent flow and heat transfer over smooth and rough walls. Good results for equilibrium boundary layer flows and for flows with separation and reattachment over a sand dune and a sand-roughened ramp are shown. Interestingly, this method allows also to take into account how roughness disrupts the viscous sublayer. This might become even more interesting, if more detailed experimental data for the near-wall region, i.e., $y^+ < 50$, of rough surfaces are available, in particular including effects of a non-small pressure gradient.

The present paper is dedicated to roughness extensions for k–ω type turbulence models which are so-called low-Re models, i.e., the momentum and turbulence model equations are integrated down to the wall. Despite recent advances in the design of wall-functions for aerodynamic flows, see e.g., Medic et al. (2005), Knopp et al. (2006), aerodynamic and turbo-machinery industry still mostly rely on low-Re models at least during the final design stage due to their very high accuracy demands. In particular for aeronautical flows, turbulence models of k–ω type and primarily the SST model by Menter (1993) and also the Spalart–Allmaras model are very popular, see e.g. Vassberg et al. (2007).

First, the well-known roughness modification by Wilcox (1998) is reviewed. Surprisingly, the validation of this model extension is very limited in literature, even in Wilcox (1998) and the cited references. Moreover, it is interesting to note that the formulation in Wilcox (1998) has been modified slightly in Wilcox (2006). In Patel and Yoon (1995), Patel (1998), some results for velocity profiles and friction factor for pipe flow and few results for fully developed channel flow are shown. Hellsten (1997) uses the roughness extension by Wilcox for two variants of the original Wilcox k–ω model, viz., the Menter BSL and the SST k–ω model, and he shows some results for boundary layers over flat plates.

The present investigation addresses two major shortcomings of this approach. The first disadvantage is the very fine near-wall mesh resolution required. Both authors Patel and Yoon (1995) and Hellsten (1997) state that for surface roughness much finer near-wall grids are required than for smooth walls. This constraint increases the computational costs for the appropriate usage of this roughness model in terms of numerical error significantly. Additionally, this can lead to severe problems for the mesh generation in complex geometries, in particular for high Reynolds number flows.

The second shortcoming is that for transitionally rough surfaces the predictions for skin friction are not fully satisfying. Both authors Patel (1998) and Hellsten (1997) consider only the case of a constant Reynolds number (based on the free-stream velocity and the length of the plate) and vary the equivalent sand grain roughness size. Instead, in the present paper the case by Ligrani and Moffat (1986) is considered, in which the roughness height is held constant and the roughness Reynolds number is changed by varying the onflow velocity. This test case is very sensitive for prediction of skin friction.

The third shortcoming is that the Wilcox roughness modification cannot be used in conjunction with the original SST model and requires an additional modification of the SST model in order to prevent the limitation of the eddy viscosity and hence of the modeled shear-stress from being activated in the near-wall region, as shown in Hellsten (1997). This may be seen as an additional indication that the roughness extension by Wilcox is not completely sound.

For these three reasons, the present paper proposes a new roughness modification for k–ω type turbulence models. The new roughness modification gives very successful predictions for a variety of validation cases including the pipe flow experiments by Nikuradse (1933) at almost the same grid resolution requirements as for smooth walls.

Surface roughness can cause separation to occur earlier. This was shown experimentally for the flow over a smoothly contoured ramp by Song and Eaton (2002), who confirmed the numerical prediction by Durbin et al. (2001). Song and Eaton (2002) conclude that the increase in skin friction and turbulence level that would be expected to delay separation are overwhelmed by the increase in the boundary layer thickness which makes the flow in the near-wall region more susceptible to separation. This test case was simulated successfully also by Suga et al. (2006). Using an analytical wall function approach in conjunction with the k-ϵ model they are able to predict the separation point and the small separation bubble in good agreement with the experiment.

An accurate prediction of the effect of surface roughness on the separation point is of great importance for aeronautical applications. In the present work, we consider the flow over an airfoil by Ljungström (1972) and Hellsten (1997), where the pressure gradient and hence the separation point can be varied by changing the incidence angle. This allows to study the sensitivity of the separation point depending on both the roughness size and the adverse pressure gradient.

The paper is organized as follows: Section 2 reviews the effects of surface roughness on the inner velocity profile. The roughness extension by Wilcox is investigated in Section 3. The new roughness modification is described in Section 4. The validation of the method for equilibrium boundary layer flows is presented in Section 5. In Section 6, the flow past an airfoil without and with surface roughness is considered and some conclusions are drawn in Section 7.

2. Roughness effects on the inner velocity profile and their modelling

In the logarithmic part of turbulent boundary layers over rough walls, the velocity profile can be described by

$$\frac{u}{u_\tau} = \frac{1}{\kappa}\ln\left(\frac{y}{k_\mathrm{r}}\right) + B, \tag{1}$$

where u_τ denotes friction velocity $u_\tau = (\tau_\mathrm{w}/\rho)^{1/2}$ with $\tau_\mathrm{w} = \rho\nu\partial u/\partial y|_\mathrm{w}$. The value of B varies with the roughness Reynolds number $k_\mathrm{r}^+ = k_\mathrm{r}u_\tau/\nu$ and is supposed to depend also on the roughness-geometry characteristics, see Ligrani and Moffat (1986). For turbulent pipe flows with sandgrain roughness, Nikuradse (1933) found experimentally that $B = 8.5$ for fully rough walls ($k_\mathrm{r}^+ \gtrapprox 70$). For hydrodynamically smooth walls ($k_\mathrm{r}^+ \lessapprox 3.5$, depending on the roughness element geometry) the classical log-law for smooth walls $u/u_\tau = \kappa^{-1}\ln(yu_\tau/\nu) + C$ is formally recovered by setting $B = \kappa^{-1}\ln(k_\mathrm{r}^+) + C$ with $C = 5.1$ in (1).

Clauser (1956) proposed to write (1) in the form

$$\frac{u}{u_\tau} = \frac{1}{\kappa}\ln\left(\frac{yu_\tau}{\nu}\right) + C - \frac{\Delta u}{u_\tau}, \tag{2}$$

where $\Delta u/u_\tau$ represents the vertical shift of the logarithmic profile caused by roughness and from (1) this shift is related to B by

$$\frac{\Delta u}{u_\tau} = C - B + \frac{1}{\kappa}\ln\left(\frac{k_\mathrm{r}u_\tau}{\nu}\right). \tag{3}$$

Based on an investigation of a variety of experimental data including Nikuradse (1933), the following curve fit for B is proposed in Ligrani and Moffat (1986)

$$B = \left[C + \frac{1}{\kappa}\ln(k_\mathrm{r}^+)\right](1 - \sin(\pi g/2)) + 8.5\sin(\pi g/2), \tag{4}$$

with interpolation function g for the transitionally rough regime

$$g = \begin{cases} \frac{\ln(k_\mathrm{r}^+/k_\mathrm{r,S}^+)}{\ln(k_\mathrm{r,R}^+/k_\mathrm{r,S}^+)}: & k_\mathrm{r,S}^+ < k_\mathrm{r}^+ < k_\mathrm{r,R}^+, \\ 1: & k_\mathrm{r}^+ > k_\mathrm{r,R}^+, \\ 0: & k_\mathrm{r}^+ < k_\mathrm{r,S}^+. \end{cases}$$

The values $k_\mathrm{r,S}^+$, $k_\mathrm{r,R}^+$ depend on the roughness-geometry characteristics. For sandgrain roughness, Ligrani and Moffat (1986) propose $k_\mathrm{r,S}^+ = 2.25$ and $k_\mathrm{r,R}^+ = 90.0$.

3. The roughness extension for k–ω type turbulence models by Wilcox

In k–ω type turbulence models, the eddy viscosity is given by $\nu_\mathrm{t} = k/\omega$, where k and ω are the solution of

$$\vec{\nabla}\cdot(\rho\vec{u}k) - \vec{\nabla}\cdot(\rho(\nu + \sigma_k\nu_\mathrm{t})\vec{\nabla}k) = 2\rho\nu_\mathrm{t}\mathbb{T}(\vec{u}) : \vec{\nabla}\vec{u} - \beta_k\rho k\omega,$$
$$\vec{\nabla}\cdot(\rho\vec{u}\omega) - \vec{\nabla}\cdot(\rho(\nu + \sigma_\omega\nu_\mathrm{t})\vec{\nabla}\omega) = 2\gamma\rho\mathbb{T}(\vec{u}) : \vec{\nabla}\vec{u} - \beta_\omega\rho\omega^2,$$

with constants $\beta_k = 0.09$, β_ω, γ, σ_k and σ_ω and

$$\mathbb{T}(\vec{u}) \equiv \mathbb{S}(\vec{u}) - \frac{1}{3}\vec{\nabla}\cdot\vec{u}\mathbb{I}, \text{ with } \mathbb{S}(\vec{u}) = \frac{1}{2}\left(\vec{\nabla}\vec{u} + (\vec{\nabla}\vec{u})^T\right).$$

In this paper, of particular interest is the SST k–ω model by Menter (1993). A central part of the SST model is the following limitation of ν_t

$$\nu_t = \min\left(\frac{k}{\omega}; \frac{a_1 k}{\Omega F_2}\right), \quad \Omega = \sqrt{2\Omega(\vec{u}) : \Omega(\vec{u})},$$
$$\Omega(\vec{u}) = \frac{1}{2}(\vec{\nabla}\vec{u} - (\vec{\nabla}\vec{u})^T), \tag{5}$$

with $a_1 = 0.31$ and F_2 being a suitable function of wall-distance which is equal to one in the viscous sublayer and in the log-layer and zero in the outer flow.

The classical roughness extension for k–ω type models by Wilcox (1998) modifies only the wall-value of ω to model effects of surface roughness

$$k|_\mathrm{w} = 0, \tag{6}$$

$$\omega|_\mathrm{w} = \frac{u_\tau^2}{\nu}S_\mathrm{R}, \quad S_\mathrm{R} = \begin{cases} (50/k_\mathrm{r}^+)^2, & k_\mathrm{r}^+ < 25, \\ 100/k_\mathrm{r}^+, & k_\mathrm{r}^+ \geqslant 25. \end{cases} \tag{7}$$

We notice that (7) has been modified slightly in Wilcox (2006).

A major drawback of this roughness modification is the very fine near-wall mesh resolution required, see also Patel and Yoon (1995), Patel (1998) and Hellsten (1997). For smooth walls, the well-known best practice guideline for mesh design states that the wall-distance of the first node above the wall in universal coordinates should satisfy $y^+(1) = 1$ if the no-slip condition is imposed, where $y^+(1) = y(1)u_\tau/\nu$ with $y(1)$ denoting the wall-distance of the first mesh node above the wall. Such a near-wall resolution is necessary for all low-Re models if the RANS equations are integrated down to the wall. Even for smooth walls, the sensitivity of the solution for k–ω models with respect to $y(1)$ is well known and deserves special attention, see e.g. Wilcox (1998). However, for rough walls, detailed numerical investigations show that for $k_\mathrm{r}^+ \lessapprox 100$, mesh convergent results are obtained only for $y^+(1) \lessapprox 0.01$. For $k_\mathrm{r}^+ \gtrapprox 100$ even smaller values for $y^+(1)$, e.g., $y^+(1) \lessapprox 0.003$ are needed in order to achieve (almost) grid converged solutions, in particular for the turbulent kinetic energy k. Patel and Yoon (1995) report that for rough surfaces the distance of the first node above the wall has to be smaller by a factor of 1000 compared to smooth walls. Patel and Yoon (1995) also report

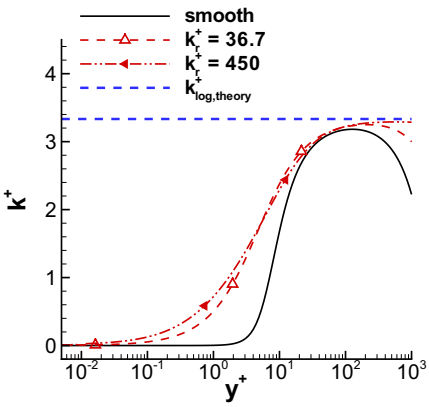

Fig. 1. Near-wall solution for turbulent kinetic energy k of the Wilcox k–ω model for flat plate turbulent boundary layer flow for smooth wall and for two different roughness Reynolds numbers k_r^+ in the transitionally and fully rough regime using the roughness extension by Wilcox.

that for rough-wall channel flow the number of nodes in wall-normal direction increases by a factor of three compared to smooth-wall calculations. In contrast, the roughness extension by Boeing for the Spalart–Allmaras model allows to use almost the same meshes as for smooth walls. Since for rough walls the sensitivity of the solution of the extended Spalart–Allmaras model on $y(1)$ is slightly more pronounced than for smooth walls, as a best practice rule we found $y^+(1) \approx 0.3$ for rough walls.

The necessity for the very small $y^+(1)$-values for rough walls is clearly seen from Fig. 1. For the smooth wall, the near-wall solution of k has zero slope until $y^+ \approx 1$. On the other hand, for rough walls a non-zero slope is discernible for $y^+ \gtrapprox 0.02$, which has to be resolved appropriately by the mesh. It should be pointed out that the numerical error on meshes designed for smooth wall calculations, i.e., with $y^+(1) = 1$, is very large and causes poor predictions for velocity and skin friction.

Moreover, it was shown in Hellsten (1997) that the Wilcox roughness modification cannot be used in conjunction with the original SST model unless F_2 in (5) is multiplied with an additional function F_3 being zero in the viscous sublayer (and one otherwise) in order to prevent the limitation of ν_t from being activated in the near-wall region. This point will be addressed in the next section.

4. New roughness extension for k–ω type turbulence models

The aim of this section is to devise a new roughness modification for k–ω type turbulence models which remedies the computationally unfavorable near-wall gradient of k arising from the Wilcox roughness modification. The new proposal is based on the ideas in Aupoix and Spalart (2003) and Durbin et al. (2001). The effect of surface roughness (1), respectively (2) can be modelled by the following ansatz for the eddy viscosity in the log-layer

$$\nu_{t,\log} = u_\tau \kappa (y + d_0). \tag{8}$$

Integration of the momentum boundary layer equation in the logarithmic region $\nu_{t,\log} \partial u/\partial y = u_\tau^2$ with the condition $u|_{y=0} = 0$ then gives

$$\frac{u}{u_\tau} = \frac{1}{\kappa} \ln\left(\frac{y + d_0}{d_0}\right). \tag{9}$$

Therein, d_0 is a hydrodynamic roughness length to be determined later and y is the wall distance. The interpretation is that the rough surface is replaced by an effective wall located at $y = 0$, defined to be where the mean velocity given by (9) is extrapolated to zero, see Durbin et al. (2001). Equating (1) and (9) then gives the following relation between d_0 and k_r

$$\frac{y + d_0}{d_0} = \frac{y}{k_r} \exp(\kappa B).$$

Using the approximation $d_0 \ll y$ for a fully rough wall by Aupoix and Spalart (2003) gives

$$d_0 = \exp(-8.5\kappa) k_r \approx 0.03 k_r. \tag{10}$$

Using the equivalent sand grain approach, under fully rough conditions, the viscous sublayer is completely disrupted. Thus, from a modelling point of view, the near-wall solution and also the wall-value of k should be close to the log-layer value corresponding to fully developed turbulent flow

$$k = u_\tau^2 / \beta_k^{1/2}, \tag{11}$$

see also Durbin et al. (2001). Although assumptions (10) and (11) cannot be strictly proven due to a lack in detailed experimental data, they will turn out to be successful modelling assumptions.

Eq. (11) implies that $\nu_t = k/\omega$ does not vanish at the wall, which can also be seen from the mixing-length approach (8). However, due to (6), the Wilcox roughness model gives $\nu_t|_w = 0$, and a large deviation in ν_t from the theoretical behaviour in the entire near-wall region is the consequence. We remark that the near-wall solution for ν_t using the SA model with Boeing roughness extension is very close to relation (8). Therefore (6) is considered to be the reason for the problems observed with the roughness extension by Wilcox.

Starting with the ansatz (11), consistency with (8) and the definition $\nu_t = k/\omega$ then implies that under fully rough conditions

$$\omega = \frac{u_\tau}{\beta_k^{1/2} \kappa (y + d_0)}. \tag{12}$$

The formula for the friction velocity u_τ has to take into account the fact that $\nu_t|_w > 0$ for rough walls and is given by

$$u_\tau^2 = \nu_{\text{eff}} \left.\frac{\partial u}{\partial y}\right|_w, \quad \nu_{\text{eff}} = \nu + \frac{k}{\omega}. \tag{13}$$

One should note that in the fully rough regime (7) and (12) evaluated at $y = 0$ differ only by a constant factor, since $d_0 = 0.03 k_r$ and (7) can be written as $\omega|_w = u_\tau/(0.01 k_r)$.

In order to achieve good predictions also for transitional roughness values, the model has to be altered. We notice the fact that the roughness extension in Aupoix and Spalart (2003) for the SA model also requires an additional modification for transitional roughness values. Relation (11) is altered to retain the condition $k|_w = 0$ for a smooth-wall by using a blending function

$$k|_w = \phi_{r1} k_{\text{rough}}, \quad k_{\text{rough}} \equiv u_\tau^2/\beta_k^{1/2}, \quad \phi_{r1} = \min\left(1, \frac{k_r^+}{90}\right). \tag{14}$$

We remark that the predictions in the transitionally rough regime are not very sensitive with respect to the special form of the blending function ϕ_{r1}.

On the other hand, the dependence of the wall value $\omega|_w$ on k_r^+ turns out to be crucial for the behaviour of the model for transitional roughness Reynolds numbers. If (12) is used without any modification, then under transitionally rough conditions two problems can be observed. Firstly, the values obtained for B, which is computed from the velocity shift $\Delta u/u_\tau$ in (2), are much larger than given by relation (4). Secondly, c_f is not increasing with increasing k_r^+ (resp. u_∞), which will be explained in detail in Section 5.1. As a remedy, we propose the following modification for $\omega|_w$ for transitional roughness values

$$\omega = \frac{u_\tau}{\beta_k^{1/2} \kappa \tilde{d}_0}, \text{ with } \tilde{d}_0 = \phi_{r2} 0.03 k_r, \tag{15}$$

where the blending function $\phi_{r2}(k_r^+)$ is given by

$$\phi_{r2} = \min\left[1, \left(\frac{k_r^+}{30}\right)^{2/3}\right] \min\left[1, \left(\frac{k_r^+}{45}\right)^{1/4}\right] \min\left[1, \left(\frac{k_r^+}{60}\right)^{1/4}\right]. \quad (16)$$

This relation is based on the observation, that for given flow conditions, increasing the wall value $\omega|_w$ gives lower predictions for c_f. Starting at the outer limit for transitional roughness, say $k_r^+ = 90$, the strategy is therefore to increase $\omega|_w$ with decreasing k_r^+ appropriately. This is achieved by the piecewise defined relation (15), (16). Thereby $\omega|_w(k_r^+)$ is designed to give monotoneously increasing c_f with increasing k_r^+ and relative changes in c_f vs. k_r^+ which are close to the experimental data by Ligrani and Moffat (1986) and close to the results for the SA model, see Section 5.1.

In order to be consistent with the limit of a hydrodynamically smooth wall, we limit $\omega|_w$ by the ω-value for a smooth wall in the boundary condition by Menter (1993)

$$\omega|_w = \min\left(\frac{u_\tau}{\beta_k^{1/2}\kappa\tilde{d}_0}, \frac{60\nu}{\beta_\omega y(1)^2}\right), \quad (17)$$

where $y(1)$ denotes the distance of the first grid point above the wall.

As a remark, the roughness modification for the SA model by Boeing does not only concern the boundary condition but also replaces the wall distance y in the destruction term for $\tilde{\nu}$ by the effective wall distance $d = y + 0.03k_r$. An analogous modification of the turbulent length scale, which appears in the destruction term of the k-equation and in the formula for ν_t, has also been investigated for the Wilcox k–ω model for fully rough surfaces, but this does not give superior results.

It is interesting to note that $\omega|_w$ from (12) is larger by a factor of 2.71 compared to the value used in (7). Regarding the SST k–ω

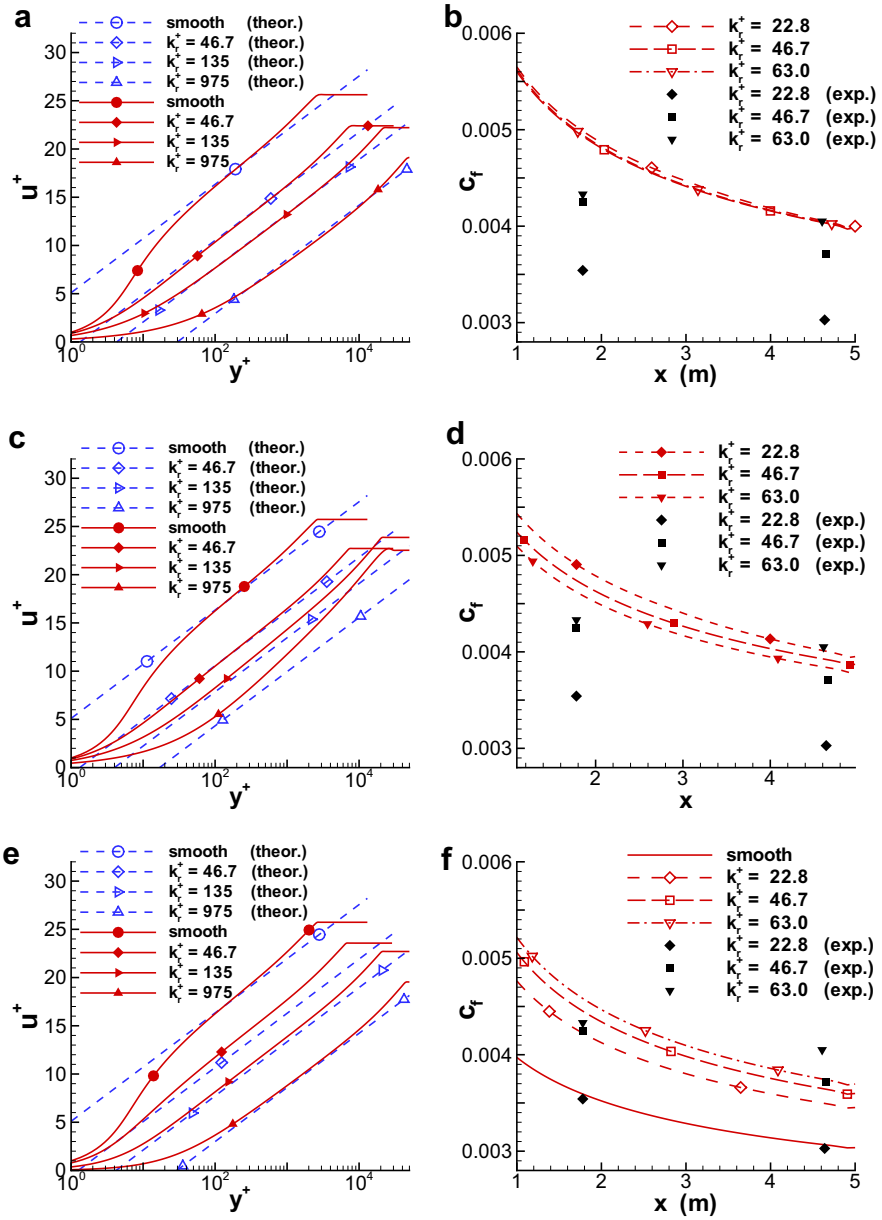

Fig. 2. Testcase Ligrani and Moffat (1986): Predictions for velocity profiles (left) and for c_f (right) for different roughness modifications and for different roughness Reynolds numbers k_r^+ (see Table 1). (a) Wilcox k–ω model with roughness extension by Wilcox on very fine meshes with $y^+(1) = 0.01$ for $k_r^+ < 100$ and $y^+(1) = 0.0025$ for $k_r^+ > 100$. (b) Wilcox k–ω model with roughness extension by Wilcox on very fine meshes with $y^+(1) = 0.01$. (c) Wilcox k–ω model with roughness extension by Wilcox on meshes with $y^+(1) = 0.3$. (d) Wilcox k–ω model with roughness extension by Wilcox on meshes with $y^+(1) = 0.3$. (e) Wilcox k–ω model with new roughness extension on meshes with $y^+(1) = 0.3$. (f) Wilcox k–ω model with roughness new extension on meshes with $y^+(1) = 0.3$.

model, as shown in Fig. 3 in Hellsten (1997), for the Wilcox roughness extension $1 < \Omega/(a_1\omega) \lessapprox 1.6$ for $1.5 < y^+ < 10$ for a fully rough surface. This causes the second term in the minimum expression in (5) to be activated in the viscous sublayer for non-small k_r^+-values, which is not intended, see Menter (1993) for the case of a smooth wall. The larger value (12) might contribute to avoid this problem, but the near wall behaviour of the velocity and hence of Ω are also of importance.

This section is concluded by a brief discussion of the approximation $d_0 \ll y$ for obtaining (10). The condition $d_0 \ll y$ can be rewritten as $d_0/y = 0.03k_r/y = 0.03k_r^+/y^+ \ll 1$ by substitution of (10). Thus one can see that the approximation is reasonable for $y^+ \gtrapprox k_r^+$. For smooth walls, according to the recent investigation by Österlund et al. (2000), the viscous influence extends within the buffer region to $y^+ \approx 200$, compared to the previously assumed limit of $y^+ \approx 50$. Regarding the question on the extent of the log-layer for rough walls it is of particular importance to take into account whether a y-origin shift is used or not, because the vertical coordinate y is often defined as $y = y' - \Delta y$, where y' is the vertical height measured from the wall and Δy is a certain fraction of the distance of the crests of the roughness elements from the base of the wall to be calibrated, see e.g. Piementa et al. (1975), Song and Eaton (2002). For transitional roughness values, the existence of a log-layer can be seen for $y^+ \gtrapprox 40$–50 from experimental data both with shift, see e.g. Fig. 2 in Ligrani and Moffat (1986) with $k_r = 0.79$ mm and $\Delta y = 0.23$ mm, and without shift, see e.g. Nikuradse (1933) which are shown in Fig. 4b in this work. For fully rough conditions at moderate k_r^+, say $k_r^+ \lessapprox 200$, the existence of a log-layer can be seen for $y^+ \geqslant 90$, see e.g. Song and Eaton (2002) (where a y-origin shift is used). On the other hand, for fully rough conditions at large k_r^+, say $k_r^+ \gtrapprox 500$ experimental data suggest that the log law does not extend down to $y^+ \approx 70 - 90$. Instead, a systematic deviation from the log-law for $y^+ < \alpha k_r^+$, with $\alpha_1 < \alpha < \alpha_2$ can be inferred from Fig. 15c–f in Nikuradse (1933), with $\alpha_1 \approx 0.5$ and $\alpha_2 \approx 0.8$. Hence, we have $y^+ \gg 0.03k_r^+$ in the region where a logarithmic law holds also for large k_r^+. Thus $d_0 \ll y$ is a reasonable approximation also for fully rough conditions even at large roughness Reynolds numbers.

It should be noted that a much more sophisticated method was devised in Durbin et al. (2001) instead of the simple relation (10). In the present paper, such a method was not used, since detailed investigations showed that for k–ω type models the calibration of the log-law shift with respect to experimental results does not necessarily imply good predictions in c_f for transitional roughness values.

5. Validation for equilibrium flows

5.1. The test case by Ligrani and Moffat

The test case by Ligrani and Moffat (1986) is a flat plate turbulent boundary layer flow over spherical roughness elements. This test case has been used to calibrate the new roughness proposal. The roughness height is held constant and the roughness Reynolds number is changed by varying the onflow velocity. The corresponding equivalent sandgrain roughness size is $k_r = 0.79$ mm according to Schlichting (1968), which was confirmed in an earlier study using fully rough velocity-profiles information, see Ligrani and Moffat (1986) and references therein. Then, by altering the free-stream velocity, transitionally rough conditions are obtained. Experimental data are available for free-stream velocities of 10.1, 15.8. 20.5, and 26.8 m s^{-1}. Additional roughness conditions for very small and very large k_r^+-values are obtained by decreasing the equivalent sandgrain roughness size k_r for the smallest onflow velocity and by increasing k_r for the largest velocity respectively. A complete list of the test conditions considered in the present numerical investigation is given in Table 1. The other data are $T_\infty = 293$ K, $\rho_\infty = 1.2$ kg m^{-3} and from Sutherland's law we obtain $\nu = \mu/\rho_\infty = 1.5 \times 10^{-5}$ m^2 s^{-1}, and the length of the flat plate is $L = 5$ m.

First the results for the roughness extension by Wilcox (6) and (7) for the Wilcox k–ω model are considered on very fine meshes with $y^+(1) = 0.01$ for $k_r^+ < 100$ and $y^+(1) = 0.0025$ for $k_r^+ > 100$ to ensure mesh convergent results. The velocity profiles together with the theoretical relation (1) and (4) are shown in Fig. 2 which are in very good agreement with the theoretical relation in the whole range of roughness Reynolds numbers. Regarding the predictions for skin friction, on the positive side, for fully rough conditions (U7–U9 in Table 1), which are at constant u_∞ and increasing k_r, the results are in fair agreement with those presented in Hellsten (1997), but not shown here. However, for transitional roughness values (cases U1–U6, see Fig. 2b) the predictions for c_f are not completely satisfying, as an almost constant level for c_f is predicted. In fact, c_f is even slightly monotoneously decreasing with increasing k_r^+. On the other hand, from the experimental data, the trend is discernible that for constant k_r, skin friction c_f is increasing with increasing u_∞, although c_f is given only at two different streamwise positions and albeit the uncertainty in the experimental results is obvious. We note that the results for the SA model with roughness extension by Boeing also exhibit such a trend.

Secondly, the results for the Wilcox roughness model are considered on meshes with $y^+(1) = 0.3$ (measured at $x = L$), motivated by the observation that the SA model with roughness extension by Boeing gives grid converged results on these meshes for all k_r^+ values in Table 1. Fig. 2c shows that the velocity profiles for large values of k_r^+ deviate largely from the profiles on the very fine meshes considered above. The large grid sensitivity of the solution with respect to $y^+(1)$ can be clearly seen from the predictions for c_f also for transitional roughness values in Fig. 2d.

Then the results for the new roughness modification are considered on meshes with $y^+(1) = 0.3$ (measured at $x = L$). The velocity profiles are shown in Fig. 2e giving good agreement with the theoretical relation in the whole range of roughness Reynolds numbers. Regarding c_f, the predicted values increase as k_r^+ is increased and both absolute levels and the relative changes in c_f are close to the experimental values, cf. Fig. 2f. We remark that for fully rough conditions (cases U7–U9), the differences in c_f between the roughness model by Wilcox and the new proposal are very small. The corresponding results are not shown here. Regarding an assessment of the predictions for c_f, it has to be kept in mind that the uncertainty regarding the experimental data for c_f is about $\pm 10\%$, see Ligrani and Moffat (1986).

Fig. 3a shows the value for B in Eq. (1) which is computed from the velocity shift $\Delta u/u_\tau$ in the logarithmic part of the boundary layer using (2) and the empirical relation (4). For the Wilcox rough-

Table 1
Summary of flow conditions in the experiment by Ligrani and Moffat (1986). The values for k_r^+ are measured at $x/L = 0.356$ and the values denoted by * are nominal values from simulations using the SA model with roughness extension by Boeing.

u_∞ $\frac{m}{s}$	10.1	10.1	10.1	10.1	15.8	20.4	26.8	39.5	60.0	90.0	90.0	90.0
k_r m	1.9	3.9	5.9	7.9	7.9	7.9	7.9	7.9	7.9	7.9	16.0	32.0
k_r^+	5*	10*	16*	22.8	36.7	46.7	63.0	89*	135*	206*	450*	975*
Name	U0b	U0a	U0	U1	U2	U3	U4	U5	U6	U7	U8	U9

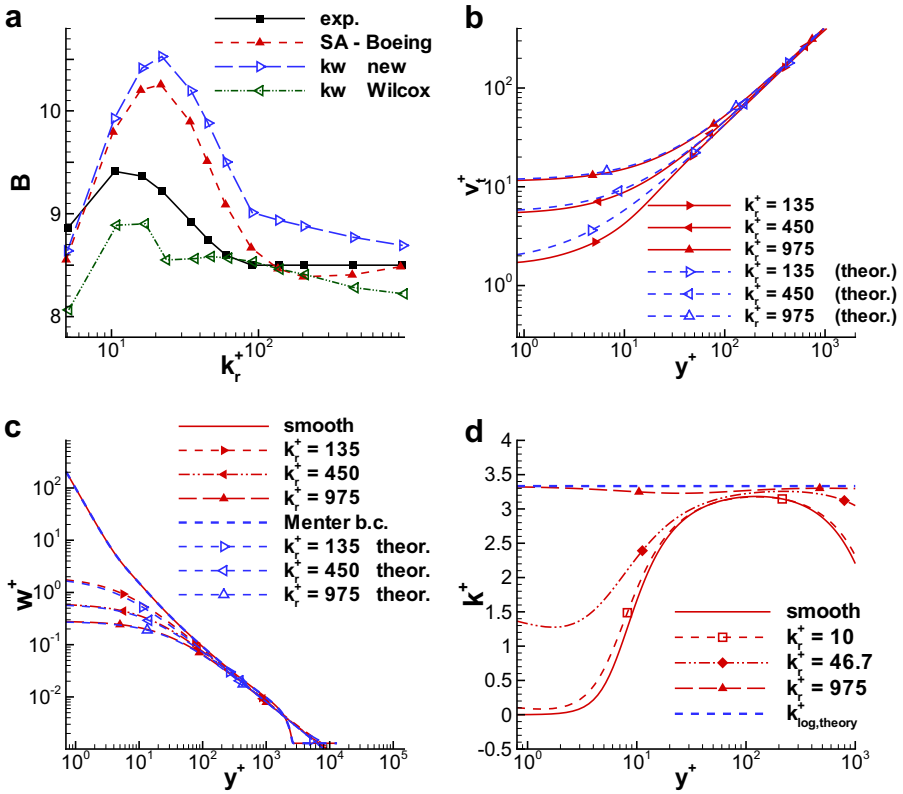

Fig. 3. Testcase Ligrani and Moffat (1986). (a) Predictions for B in Eq. (1) computed from the velocity shift $\Delta u/u_\tau$ in (2). Each symbol denotes a pair (k_r^+, B) for a certain flow condition in Table 1. (b) Prediction for v_t and relation (8) for the Wilcox k–ω model with new roughness extension. (c) Prediction for ω and relation (12) for the Wilcox k–ω model with new roughness extension. (d) Prediction for k and relation (11) for the Wilcox k–ω model with new roughness extension.

ness model the results on the very fine mesh are considered. Each symbol denotes the prediction for the pair (k_r^+, B) for a certain flow condition in Table 1. The new roughness modification and the SA model overpredict the value of B for transitional roughness values k_r^+. On the other hand, the Wilcox roughness modification slightly underpredicts the variation of B with varying k_r^+. However, for the Wilcox roughness modification the values of k_r^+ and hence u_τ are little overpredicted for transitional roughness values compared to the experimental data in a way such that the predictions for c_f are almost constant. From this observation we conclude that at least for k–ω type models a reasonable prediction of the log-layer shift for the velocity profiles does not necessarily imply good predictions for c_f. Hence the new proposal was designed as a compromise to achieve reasonable results for both c_f and B. Skin friction is determined also by the near-wall behaviour of velocity. But the question of how roughness has the effect of disrupting the viscous sublayer goes beyond the equivalent sand grain approach. Moreover, to the author's best knowledge, the available experimental data regarding this issue are very limited.

Finally, we mention that the predictions for c_f using the SST k–ω model are very similar to the results for the Wilcox k–ω model but they are not shown here. Regarding the cases in Table 1, the second term in the minimum expression of (5) is activated in the region $y^+ < 12$ only for the small roughness Reynolds numbers $k_r^+ \leqslant 22.8$. But it exceeds the first term by less than 2% which has no visible influence on the prediction of c_f. For all larger k_r^+-values, it remains deactivated. Therefore no additional modification of the SST model is needed for the present roughness extension, in contrast to the roughness extension by Wilcox.

This section is concluded by investigating the near-wall behaviour of the turbulence quantities k, ω and the eddy viscosity v_t. Obviously, the behaviour in v_t is close to the theoretical relation (8) for fully rough conditions, see Fig. 3b. Fig. 3c shows the solution for ω for different k_r^+ values. In the fully rough regime, the near-wall behaviour of ω is close to (12). The near-wall behaviour for k is shown in Fig. 3d demonstrating that the new roughness model remedies the near-wall gradient of k appearing for the Wilcox roughness modification. In the fully rough regime, k is very close to its log-layer value (11) in the entire near-wall region down to the wall.

A detailed comparison for other testcases, for which experimental data exist, is presented in the following sections.

5.2. Experiments by Nikuradse

In this section, we consider the experiments by Nikuradse (1933) for fully developed flow in pipes of various roughnesses. Six roughness levels are investigated in two Reynolds number areas, see Tables 2 and 3. The tables also summarize the predictions for the roughness Reynolds number k_r^+ and the quantity B which describes the shift in the log-law of the velocity profiles. Therein R denotes the radius of the pipe. The accuracy in the predictions for skin friction coefficient, respectively friction factor can be inferred directly from the agreement in k_r^+.

For the high Reynolds numbers of Table 2, the new roughness modification for k–ω type models applied to the Wilcox k–ω model predicts k_r^+ and B in good agreement with the experimental data. Additionally, the predictions for the SA model with roughness extension by Boeing are shown for comparison. The results for the roughness modification by Wilcox on the meshes used with $y^+(1) \approx 0.2$ are also shown. It can be clearly seen that for roughness Reynolds numbers greater than hundred the results are poor.

The velocity profiles for the high Reynolds numbers are shown in Figs. 4a and c. The new roughness modification applied to the

Table 2
Summary of flow conditions of the Nikuradse experiments at high Reynolds numbers using the SA model and the Wilcox k–ω model on meshes with $y^+(1) \approx 0.2$.

$\frac{R}{k_r}$	Re	k_r^+ exp.	k_r^+ SA	k_r^+ new	k_r^+ Wilcox	B exp.	B SA	B new	B Wilcox
15	4.30×10^5	1230.27	1201.2	1205.2	938.62	8.6	8.61	8.66	14.12
30.6	6.38×10^5	805.38	792.9	790.9	678.08	8.5	8.5	8.65	13.8
60	6.77×10^5	369.83	364.2	364.9	329.9	8.44	8.51	8.65	12.6
126	9.60×10^5	229.61	223.35	223.3	202.15	8.38	8.5	8.65	12.01
252	6.24×10^5	66.98	64.25	62.1	62.22	8.6	8.89	9.30	9.10
507	5.07×10^5	48.53	48.47	47.8	48.25	8.68	9.21	9.68	9.05

Table 3
Summary of flow conditions of the Nikuradse experiments at medium Reynolds numbers using the SA model and the Wilcox k–ω model on meshes with $y^+(1) \approx 0.3$.

$\frac{R}{k_r}$	Re	k_r^+ exp.	k_r^+ SA	k_r^+ new	k_r^+ Wilcox	B exp.	B SA	B new	B Wilcox
15	4.3×10^4	124.45	115.05	119.6	119.58	8.44	8.52	8.65	9.15
30.6	4.3×10^4	52.48	49.01	50.76	50.8	8.7	9.03	9.5	9.14
60	7.0×10^4	37.49	36.5	34.94	35.47	9.09	10.2	10.2	9.12
126	5.05×10^4	11.09	10.89	10.8	11.04	9.55	9.73	9.8	9.10
252	5.1×10^4	5.34	5.36	5.34	5.41	9.1	8.6	9.1	8.55
507	4.9×10^4	2.5	2.547	2.514	2.49	7.8	7.2	7.75	7.6

Wilcox k–ω model and the SST model demonstrate good agreement with the experimental data. The shift of the log-law is well matched, except for $R/k_r = 507$, where a moderate deviation in B can be observed, albeit the predictions for k_r^+ are close to the experiment. For small wall distances y, i.e., for $\frac{y}{R} \leqslant 0.2$, all models give predictions close to the experiments, and the differences become larger near the pipe center. The predictions for the SST model are close to the Wilcox model for large roughness Reynolds numbers, see Fig. 4c, albeit a small deviation from the results for the Wilcox k–ω model is discernible for $R/k_r = 60$ for transitional roughness, see Fig. 4d.

The flow conditions for the medium Reynolds number experiments are given in Table 3. Simulations are performed on meshes with $y^+(1) \approx 0.3$. For k_r/R smaller than 1/30.6, transitional roughness values can be observed. The result for the roughness extension by Wilcox deviates significantly from the experimental value for the largest k_r^+ value, in agreement with the observations for the high Reynolds number experiments in Table 2. For the new roughness extension, the predictions for the velocity profiles are shown in Figs. 4b and d. The agreement with the experimental results is good for all roughness values, except for $R/k_r = 60$, where friction is little underestimated by all models. Therefore, the corresponding

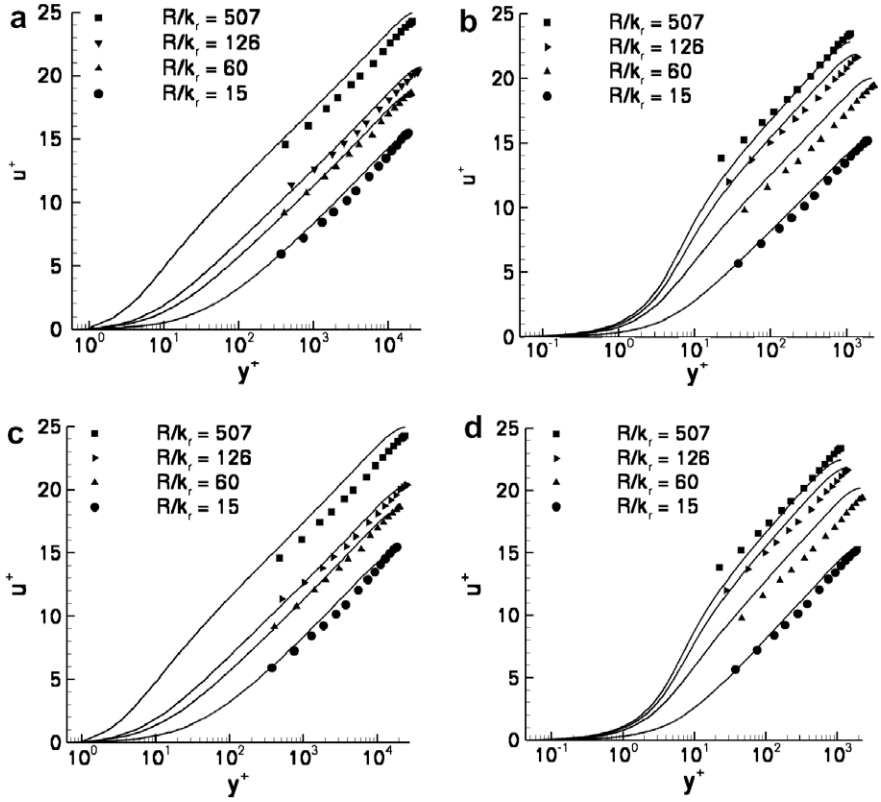

Fig. 4. Nikuradse experiments (1933). Left: Predictions for velocity profiles at high *Re*, see Table 2. Right: Predictions at medium *Re*, see Table 3. (a) Wilcox k–ω model with new roughness extension at high *Re*. (b) Wilcox k–ω model with new roughness extension at medium *Re*. (c) SST k–ω model with new roughness extension at high *Re*. (d) SST k–ω model with new roughness extension at medium *Re*.

log-layer velocity profiles in wall coordinates show a higher level than the experimental data.

5.3. Experiment by Blanchard

We consider the zero pressure gradient flow over a rough surface by Blanchard (1977). The average height of the sand grain paper is 0.425 mm from which Blanchard proposed the value $k_r = 0.85$ mm for the equivalent sand grain roughness. The onflow velocity is 45 m s^{-1} and we used $L = 0.8$ m.

In this subsection the Wilcox k–ω model is used. Regarding the mesh design, $y^+(1) \approx 0.4$ for the SA roughness extension and the new proposal, whereas for the Wilcox roughness modification $y^+(1) = 0.008$, both measured at $x/L = 1$. For this case the roughness extension by Boeing was used with the SA model version by Edwards and Chandra (1996). Fig. 5 shows the predictions for c_f. All models predict an increase of c_f compared to the smooth flat plate, where the SA model yields closest agreement with the experimental data. The new roughness extension gives slightly larger c_f values which can already be observed to a smaller extent for the smooth wall. Nevertheless, this effect is smaller than with the Wilcox roughness modification which yields the highest c_f values. Notice that for the SA model, the predictions for c_f are close to the results presented in Aupoix and Spalart (2003), Fig. 1.

5.4. Experiments by Hosni et al.

In this section, we consider the turbulent boundary layer flow over a rough surface of length $L = 2.4$ m composed of hemispheres of diameter $l_0 = 1.27$ mm investigated experimentally in Hosni et al. (1991, 1993). The roughness elements are arranged in staggered arrays and the spacing l_1 of two roughness elements is given by $l_1/l_0 = 2$, see Fig. 1 in Hosni et al. (1993). Following Aupoix and Spalart (2003), the equivalent sand grain roughness k_r is computed from the empirical formula in Dirling (1973)

$$k_r = \alpha k_{r,m}, \quad \alpha = \begin{cases} 0.0164\Lambda^{3.78}; & \Lambda < 4.93, \\ 139.0\Lambda^{-1.90}; & \Lambda > 4.93, \end{cases}$$

$$\Lambda = \frac{l_1}{k_{r,m}} \left(\frac{A_p}{A_s}\right)^{-4/3},$$

where $k_{r,m}$ is the mean roughness element height, l_1 is the mean distance between roughness elements, A_p/A_s is the ratio of roughness element surface projected on a plane normal to the flow direction to the roughness element windward surface area. The ratio A_p/A_s depends on the geometry of the roughness element type with $A_p/A_s = 0.5$ for hemispheres. For $l_1/k_{r,m} = 4$ we obtain $k_r = 1.0946 \times 10^{-3}$ m.

Testcase MSU1 (onflow velocity 12 ms^{-1}) shows transitional roughness values $k_r^+ \approx 40$ at streamwise position $x = 2$ m. The corresponding predictions for c_f are given in Fig. 6 (left). For testcase MSU2 (onflow velocity 58 ms^{-1}) fully rough conditions are obtained with $k_r^+ \approx 200$ at streamwise position $x = 2$ m. The experimental data show a significant spreading for case MSU2. Concerning the mesh design, $y^+(1) \approx 0.3$ for the SA roughness extension and the new proposal, whereas for the Wilcox roughness modification $y^+(1) = 0.01$ for case MSU1 and $y^+(1) = 0.006$ for case MSU2, all measured at $x/L = 1$. For this case the roughness extension by Boeing was used with the SA model version by Edwards and Chandra (1996). Moreover, the Wilcox k–ω model was used. For both cases MSU1 and MSU2, the SA model with roughness extension predicts the smallest increase in c_f and the Wilcox roughness modification predicts the largest increase in c_f, which is similar to the observation for the testcase by Blanchard (1977). The predictions for c_f for the new proposal are between the SA model and the Wilcox roughness modification. For case MSU1, the predictions for the roughness modification by Wilcox are in closest agreement with the experimental data, see Fig. 6 (left). For case MSU2, the SA model shows the smallest deviation to the experimental data, see Fig. 6 (right). We remark that for both cases the results for c_f by the SA model are close to those presented in Aupoix and Spalart (2003).

It is worthwhile mentioning that for both cases the uncertainty in c_f is estimated to be about ±10–12% by Hosni et al. (1993). Moreover it has to be pointed out that k_r is determined using the empirical relation by Dirling (1973), which shows a considerable uncertainty when compared with experimental data, see Fig. 2 in Dirling (1973). Thus, the spreading in the predictions for c_f of the different roughness modifications is of the same order of magnitude as the uncertainties of the experimental data and the value of k_r.

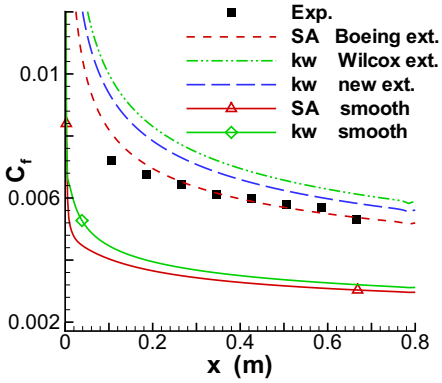

Fig. 5. Testcase by Blanchard: Prediction for c_f using the SA model and the Wilcox k–ω model.

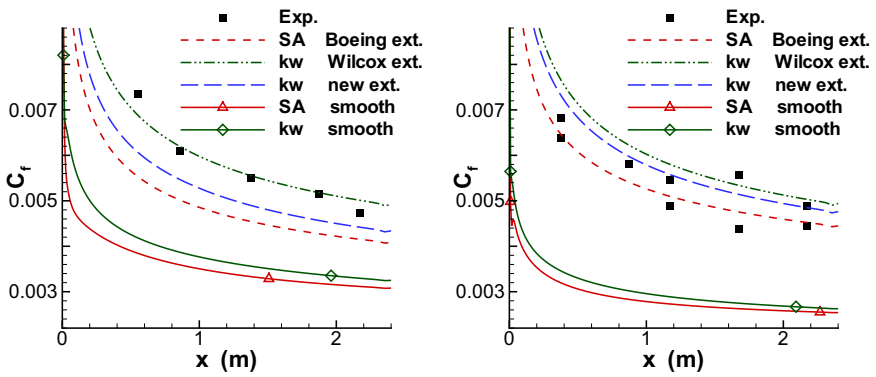

Fig. 6. Testcase by Hosni: prediction for c_f for MSU1 (left) and for MSU2 (right) using the Wilcox k–ω model.

6. Flow past an airfoil with surface roughness

In this section the method is applied to the flow past a NACA 65_2215 airfoil. For the smooth airfoil, experimental data can be found in Abbott and von Doenhoff (1959). Regarding the case with surface roughness, an experimental study has been made for the NACA 65_2A215 airfoil by Ljungström (1972), which is very close to the NACA 65_2215 airfoil, cf. Hellsten (1997). This test case has also been considered by Bragg et al. (1986) and Hellsten (1997).

The flow conditions considered here are for Reynolds number $Re = 2.6 \times 10^6$ (based on the chord length $c = 1$[m]) and Mach number $Ma = 0.182$. The roughness covers the entire upper surface and the lower surface from the leading edge to $x/c = 0.15$. In this work, we consider two cases with corresponding equivalent sandgrain size $k_r/c = 1.54 \times 10^{-4}$ and $k_r/c = 3.08 \times 10^{-4}$, which are suggested from the sand-paper characteristics by Bragg et al. (1986). Both k_r values correspond to transitionally rough conditions.

The strong adverse pressure gradient on the upper side causes the turbulent boundary layer to separate, as sketched in Fig. 7a. This test case was intended to study the effect of rime ice on the airfoil performance and allows to investigate the effect of surface roughness when increasing the adverse pressure gradient by increasing the angle of attack of the airfoil.

The computational mesh is of hybrid type. A prismatic mesh is used near the airfoil for a proper treatment of boundary layers. In order to ensure grid converged results also in the region of adverse pressure gradient and separated flow, a relatively fine prismatic mesh is chosen, i.e., 46 prismatic layers with a spacing of $\Delta y/c = 1.5 \times 10^{-6}$ for the first off-wall node, which corresponds to $y^+(1) \sim 0.25$ in the leading edge region on the upper side. In the region above the airfoil and in the wake the tetrahedral mesh is refined in order to resolve the flow accurately also in case of separation. For smaller angles of attack, computations were performed using the steady state solver. For larger angles of attack, a time-accurate integration was used until steady state solutions were obtained. For the largest incidence angles, i.e., beyond maximum lift, flow becomes slightly unsteady and the time dependent lift coefficient c_l performs oscillations with an amplitude of at most 1% in c_l. Then the time-averaged mean value for c_l was taken.

The SST k–ω model is used instead of the standard Wilcox k–ω model because the SST model is known to give superior results for flows with separation, see Menter (1993). Fig. 7b shows the predic-

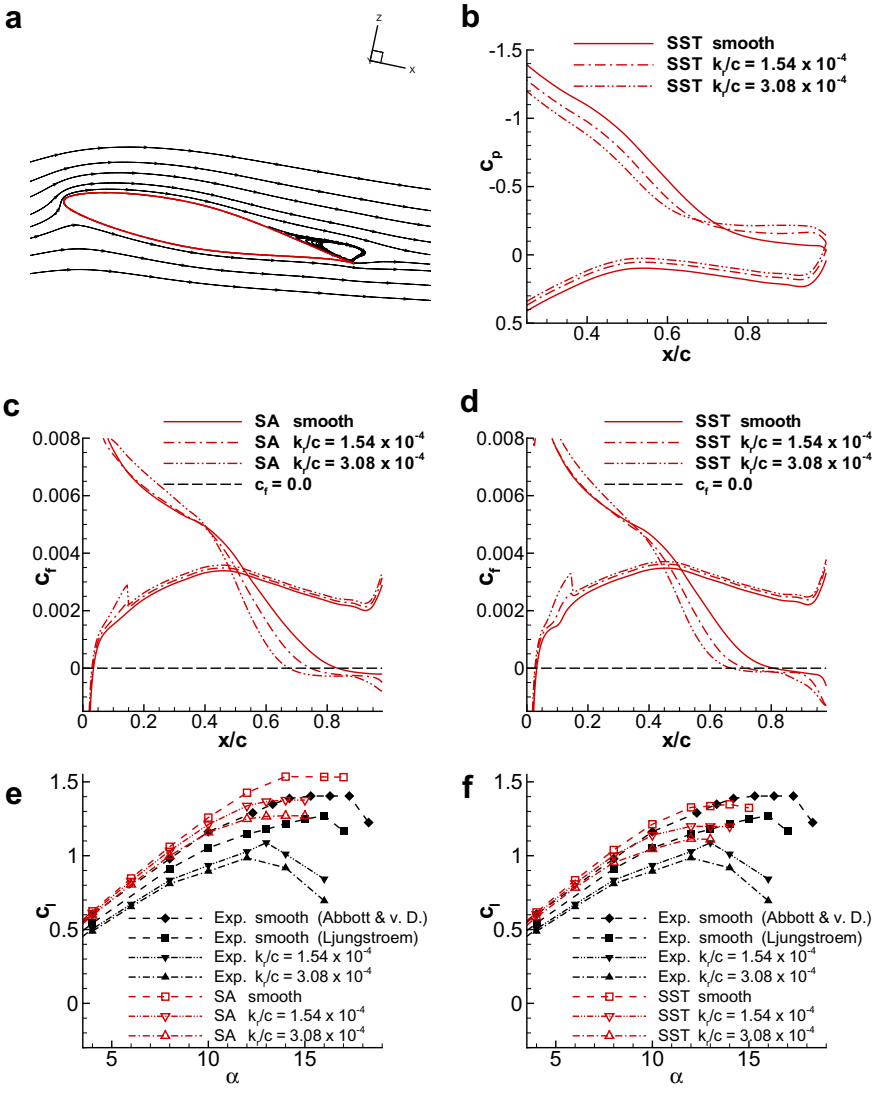

Fig. 7. Flow past NACA 65_2215 airfoil without and with surface roughness. (a) Streamlines for $\alpha = 12^\circ$, $k_r/c = 1.54 \times 10^{-4}$ using SST k–ω model. (b) C_p for SST k–ω model with new roughness extension ($\alpha = 12^\circ$) near the trailing edge. (c) C_f for SA model with roughness extension by Boeing ($\alpha = 12^\circ$). (d) C_f for SST k–ω model with new roughness extension ($\alpha = 12^\circ$). (e) C_l vs. α for SA model with roughness extension by Boeing. (f) C_l vs. α for SST k–ω model with new roughness extension.

tion for the pressure coefficient c_p for the SST k–ω model for $\alpha = 12^\circ$. Unfortunately no experimental data for c_p are available. As $-c_p$ is plotted, the upper part of the curve corresponds to the upper side of the airfoil, whereas the lower part of the curve corresponds to the lower side of the airfoil. Near the trailing edge ($x/c = 1$), a pressure plateau is discernible, which is well-known to indicate a region of separated flow. It can be seen that the pressure plateau becomes larger and more pronounced with increasing surface roughness.

Fig. 7c and d shows the prediction for skin friction c_f for the SA model and for the SST k–ω model. The lower curve corresponds to the lower side of the airfoil, where the abrupt variation in c_f due to the change from rough to smooth surface at $x/c = 0.15$ can be clearly seen. The upper curve corresponds to the upper side of the airfoil. The separation point is where $c_f = 0$. For both models, qualitatively the same result can be observed. Surface roughness causes a larger c_f near the leading edge. But subsequently, skin friction declines more steeply than on a smooth wall and flow separation occurs earlier. This effect becomes more pronounced when roughness is increased. This result is in full agreement with the results in Durbin et al. (2001) and Suga et al. (2006) and with the experiment by Song and Eaton (2002).

Finally, the effect of surface roughness on the predictions for the integral lift coefficient c_l is considered, which is the quantity of major engineering interest. Fig. 7e and f shows the lift coefficient c_l versus angle of attack α for the SA model and for the SST k–ω model. The experimental data by Ljungström (1972) are also shown for comparison and also the data by Abbott and von Doenhoff (1959) for the smooth NACA 65_2215. According to Hellsten (1997) the difference in maximum lift coefficient for the smooth airfoil is about 11% in the experiments but only a difference of about 3% should be expected from the small changes in airfoil geometry between the NACA 65_2A215 and the NACA 65_2215. Therefore Hellsten (1997) concludes that the lift coefficients by Ljungström (1972) are too low, probably due to geometrical imperfection arising from a retracted flap in his experiments.

Before considering the numerical predictions, it has to be pointed out that the accurate prediction of the absolute value of maximum lift is still an open problem at the present state of statistical turbulence modelling despite the advances during the past decades. The SA model predicts the relative changes in c_l with increasing surface roughness in good agreement with the experimental data. However, the absolute level in predicted c_l is too large when taking into account a correction of the experimental data by Ljungström (1972) based on the data by Abbott and von Doenhoff (1959). This stems from a too late prediction of the separation point. On the other hand, for the SST k–ω model with the new roughness extension both the relative changes and the absolute level in predicted c_l show a remarkably good agreement with the experimental data if the experimental data are corrected in the sense above. It can be seen from Fig. 7d that the SST k–ω model predicts the separation point earlier than the SA model which is seen to be the reason for the better predictions in c_l. This demonstrates the importance of using a two-equation turbulence model like the SST k–ω model for predicting flows with separation induced by an adverse pressure gradient and relevance to provide a suitable roughness extension for such models. This is of fundamental importance to predict the performance of airfoils and turbine blades without and with surface roughness also at the boundary of their operative range where stall may occur.

7. Conclusion

A new extension for k–ω type turbulence models to account for surface roughness has been presented which allows for the simulation of flows over rough surfaces at the same grid resolution requirements as for smooth walls. Thereby the extremely fine near-wall mesh resolution required by the Wilcox roughness modification is avoided which significantly constrains the applicability of the Wilcox roughness modification for flows at high Reynolds numbers in complex geometries. Moreover the reason for this grid restriction is revealed. Secondly the new roughness modification gives significantly improved predictions in skin friction for transitional roughness Reynolds numbers compared to the roughness extension by Wilcox. Thirdly, the new roughness extension does not require a modification of the SST k–ω model by Menter (1993), whereas a modification is necessary if the roughness extension by Wilcox is used. For equilibrium boundary layer flows the predictions of the new roughness modification are in close agreement with the results for the roughness extension by Boeing for the Spalart–Allmaras turbulence model and with experimental data for a variety of test cases in the entire roughness Reynolds number range. Moreover, the results are very close to the roughness modification by Wilcox for fully rough surfaces. Finally, the new method has been applied successfully to predict the aerodynamic effects of surface roughness on the flow past an airfoil in highlift conditions for a variety of angles of attack corresponding to different situations of adverse pressure gradient without and with separation. In particular the SST model predicts the maximum lift and the effects of surface roughness on the maximum lift in better agreement with the experimental data than the SA model. This demonstrates the importance of a suitable roughness formulation for two-equation turbulence models of k–ω type, e.g., the SST model, to predict the performance of airfoils and turbine blades without and with surface roughness also at the boundary of their operative range where stall may occur.

Future work is on the extension of the method for heat transfer. Moreover, it is planned to apply the method to flows around airfoils with glaze and rime icing, where the process of ice formation should be included in the simulations.

Acknowledgements

This work was partially funded by AIRBUS, which is gratefully acknowledged. The author is grateful to Drs. Christian Bartels and Thomas Gerhold for valuable discussions and to Drs. Bertrand Aupoix and Phil Ligrani for valuable information and assistance regarding the experimental data. Special thanks are to Dr. Klaus Becker. Finally the valuable comments and suggestions of the referees and the editor are gratefully acknowledged.

References

Abbott, I.H., von Doenhoff, A.S., 1959. Theory of Wing Sections. Dover Publications, New York.

Aupoix, B., Spalart, P.R., 2003. Extensions of the Spalart–Allmaras turbulence model to account for wall roughness. International Journal of Heat and Fluid Flow 24, 454–462.

Blanchard, A., 1977. Analyse Expérimentale et Théorique de la Structure de la Turbulence d'une Couche Limite sur Paroi Rugueuse. Ph.D. thesis, Université de Poitiers U.E.R.-E.N.S.M.A.

Bragg, M.B., Gregorek, G.M., Lee, J.D., 1986. Airfoil aerodynamics in icing conditions. Journal of Aircraft 23, 76–81.

Clauser, F.H., 1956. The turbulent boundary layer. Advances in Applied Mechanics 4, 1–51.

Dirling, R.B., 1973. A method for computing rough wall heat transfer rates on reentry nosetips. AIAA Paper 1973-763.

Durbin, P.A., Medic, G., Seo, J.M., Eaton, J.K., Song, S., 2001. Rough wall modification of two layer k–ϵ. Journal of Fluids Engineering – Transactions of the ASME 123, 16–21.

Edwards, J.R., Chandra, S., 1996. Comparison of eddy viscosity-transport turbulence models for three-dimensional, shock separated flowfields. AIAA Journal 34, 756–763.

Hellsten, A., 1997. Extension of the k–ω-SST turbulence model for flows over rough surfaces. AIAA Paper 1997-3577.

Hosni, M.H., Coleman, H.W., Taylor, R.P., 1991. Measurements and calculations of rough-wall heat transfer in the turbulent boundary layer. International Journal of Heat and Mass Transfer 34, 1067–1082.

Hosni, M.H., Coleman, H.W., Garner, J.W., Taylor, R.P., 1993. Roughness element shape effects on heat transfer and skin friction in rough-wall turbulent boundary layers. International Journal of Heat and Mass Transfer 36, 147–153.

Kays, W.M., Crawford, M.E., 1993. Convective Heat and Mass Transfer, third ed. McGraw-Hill, New York.

Knopp, T., Alrutz, T., Schwamborn, D., 2006. A grid and flow adaptive wall-function method for RANS turbulence modelling. Journal of Computational Physics 220, 19–40.

Ligrani, P.M., Moffat, R.J., 1986. Structure of transitionally rough and fully rough turbulent boundary layers. Journal of Fluid Mechanics 162, 69–98.

Ljungström, B., 1972. Wind tunnel investigations of simulated hoar frost on a 2-dimensional wing section with and without high lift devices. Technical Report, Aeronautical Research Institute of Sweden, FFA, Report AU-902.

Medic, G., Kalitzin, G., Iaccarino, G., van der Weide, E., 2005. Adaptive wall functions with applications. AIAA Paper 2006-3744.

Menter, F.R., 1993. Zonal two equation k/ω turbulence models for aerodynamic flows. AIAA Paper 1993-2906.

Nikuradse, J., 1933. Strömungsgesetze in rauhen Rohren. Technical Report, VDI-Forschungsheft 361, Berlin.

Österlund, J.M., Johansson, A.V., Nagib, H.N., Hites, M.H., 2000. A note on the overlap region in turbulent boundary layers. Physics of Fluids 12, 1–4.

Patel, V.C., 1998. Perspective: flow at high reynolds number and over rough surfaces – Achilles heel of CFD. Journal of Fluids Engineering – Transactions of the ASME 120, 434–444.

Patel, V.C., Yoon, J.Y., 1995. Application of turbulence models to separated flow over rough surfaces. Journal of Fluids Engineering – Transactions of the ASME 117, 234–241.

Piementa, M.M., Moffat, R.J., Kays, W.M., 1975. The turbulent boundary layer: an experimental study of the transport of momentum and heat with the effect of roughness. Technical Report, Report No. HMT-21, Thermosciences Division, Department of Mechanical Engineering, Stanford University.

Schlichting, H., 1968. Boundary Layer Theory, sixth ed. McGraw-Hill.

Song, S., Eaton, J.K., 2002. The effects of wall roughness on the separated flow over a smoothly contoured ramp. Experiments in Fluids 33, 38–46.

Suga, K., Craft, T.J., Iacovides, H., 2006. An analytical wall-function for turbulent flows and heat transfer over rough walls. International Journal of Heat and Fluid Flow 27, 852–866.

Vassberg, J.C., Tonico, E.N., Mani, M., Brodersen, O.P., Eisfeld, B., Wahls, R., Morrison, J.H., Zickuhr, T., Laflin, K.R., Mavriplis, D., 2007. Summary of the third AIAA CFD drag prediction workshop. AIAA Paper 2007-0260.

Wilcox, D.C., 1998. Turbulence modeling for CFD, second ed. DWC Industries, La Canada.

Wilcox, D.C., 2006. Turbulence Modeling for CFD, third ed. DWC Industries, La Canada.